

## **An electrochemical sensor based on a graphene/AuNP nanocomposite for the determination of prolyl hydroxylase**

*Lintao Jiang, Qinghao Guo, Shijiang Yang and Jun Cai\**

Department of Emergency and Trauma Surgery, The Central Hospital of Wuhan, Tongji Medical College, Huazhong University of Science and Technology. Wuhan, Hubei, 430014, P.R. China

\*E-mail: [caijunclcj@sina.com](mailto:caijunclcj@sina.com)

*Received: 24 November 2017 / Accepted: 16 January 2018 / Published: 10 April 2018*

---

Prolyl hydroxylase (PHD1) is a vital indicator of a patient's health level evaluation after liver metastases. The present study reports the fabrication of a state-of-the-art and highly conductive graphene-gold nanoparticle-modified glassy carbon electrode (GCE-graphene-AuNPs) for application in PHD1 analysis. Fabrication of the composite was achieved by the successive electrodeposition of Au NPs and graphene onto the GCE surface. It was found that the oxidization was a diffusion-controlled, irreversible process over a pH range of 3.0 to 10. Over a paclitaxel concentration range of 0.01 to 2 mM, a linear relationship was found between the concentration and the anodic peak current. Additionally, the limit of detection (LOD) was calculated as 0.004 mM.

---

**Keywords:** Electrochemical determination; Prolyl hydroxylase; Graphene; Au nanoparticle; Liver injury

### **1. INTRODUCTION**

To date, the only curative treatment of colorectal liver metastases (CRLM) is surgical resection, but the resection extent is limited by the function of the remaining liver [1-3]. Presently, systematic routes are used for the stimulation of liver regeneration, including portal vein embolization or ligation (PVL), along with associated liver partition and PVL (ALPPS). Unfortunately, postresectional liver failure occurs in as many as 9.1% of patients that undergo extended liver resection [4, 5], which necessitates the development of new strategies for liver regeneration stimulation. In surgically relevant settings, prolyl hydroxylases (PHDs) are gaining increasing attention due to their ability to initiate the degradation of HIFs in normoxia [6]. Pharmacologic inhibition of PHD enzymes can be realized by substituting essential cofactors or by targeting their catalytic site. As confirmed by a phase 1

investigation, pharmacological PHD inhibitors can be safely administered in humans, and larger phase 2 and 3 trials are in progress [7-9].

Considering the enhancement effect of the genetic PHD1 deficiency on liver regeneration and hypoxia tolerance in mice, the inhibition of PHD1 is a potential method when treating CRLM patients in need of extended pHx. However, the stabilization of HIF is related to undesirable prognosis and aggressiveness in tumors [10, 11]. In addition, in terms of colorectal cancer (CRC), the association of PHD enzymes with tumor-suppressive effects has been reported. Therefore, specific effects of PHD inhibition on tumor growth must be clinically determined, which necessitates clinical PHD1 analysis for diagnostics [12, 13]. Recently, many different studies have been reported on graphene, both in technology and science fields. Due to graphene's distinct physicochemical features, including strong mechanical strength, high electric conductivity, high thermal conductivity, and high surface area (theoretically 2630 m<sup>2</sup>/g for single-layer graphene), this material has been extensively used in applications such as electronics, energy storage and conversion (supercapacitors, batteries, fuel cells, solar cells) [14-20]. Graphene and its composites can potentially be used in the preparation of electrochemical biosensors, considering their mass production, easy functionalization, distinct biocompatibility, low noise, and favorable conductivity. Unfortunately, due to its hydrophobic property, functionalization of graphene using chemical groups is necessary for better feasibility [21-23], which involves a range of chemical reactions along with sophisticated control of the conditions. The electrodeposition technique is characterized by eco-friendliness and convenience. The reduction of graphene oxide in a dispersion into graphene occurs during electrodeposition, which is followed by direct deposition on the surface of the electrode [24-27].

A commonly used method of biomolecule analysis is the modification of an electrode by graphene-gold nanoparticles through deposition of the gold nanoparticles (AuNPs) [28-30]. Gold nanoparticles have often been reported as being biocompatible with biomolecules; meanwhile, graphene does not exert much influence on biomolecule bioactivity due to its inertness. Therefore, the synergy between these two materials enables the electrode to be distinctly biocompatible with affinity for biomolecules [31-33]. Additionally, the electrode is much more conductive after the electrodeposition of the graphene-gold nanoparticles that serve as an electron mediator.

This report proposes a cost-effective and facile current voltammetric route for PHD1 analysis based on the electrochemical oxidation of PHD1 using a graphene-AuNP-modified electrode. On the other hand, an electroanalytical strategy was used for PHD1 analysis under optimum parameters. Our proposed method is easily repaired, rapid in response, highly reproducible, characterized by PHD1itaxel renewal, and has a low limit of detection (LOD), and this method was further used for the detection of serum PHD.

## 2. EXPERIMENTS

### 2.1. Materials

Pure PHD1 (powder), a gift from Reddy's Laboratory (Hyderabad) was used without further purification. Graphite oxide was commercially available from XF Nano Inc. (Nanjing, China). All reagents were of analytical grade. Electrochemical experiments were performed on a CHI760D

electrochemistry system (Chenhua Instrument, Shanghai, China) with a three-electrode geometry, where the working, auxiliary, and reference electrodes were a 3-mm diameter glassy carbon electrode (GCE), a Pt foil, and a saturated calomel electrode (SCE), respectively. Other devices used in our case included a Model CS501-SP thermostat (Huida Instrument, Chongqing, China), a Sigma 4K15 laboratory centrifuge, a Sigma 1–14 Microcentrifuge (Sigma, Germany), and an AFS-9700 atomic fluorescence spectrophotometer (Kechuang Haiguang Instrument, Beijing, China). Unless otherwise stated, all experiments were carried out at ambient temperature (25 °C).

## 2.2. Sensor fabrication

The sensor was prepared by the electrodeposition of Au and graphene on the surface of a GCE pre-treated with  $\text{H}_2\text{SO}_4$ , followed by the self-assembly of a thiolated P1 on the GCE. A colloidal dispersion of graphene oxide (1.0 mg/mL) was prepared by adding graphite oxide powder into pH 9.18 phosphate-buffered saline (PBS), and then exfoliating under ultrasonication. The as-prepared dispersion was subjected to reduction using cyclic voltammetry (CV) at 10 mV/s under magnetic stirring and  $\text{N}_2$  bubbling at 4 °C over an applied potential range of  $-1.5$  to  $0.5$  V. This was followed by the electrodeposition of Au onto the graphene-coated GCE at  $0.18$  V in a  $\text{HAuCl}_4$  solution (1%, w/w) containing  $0.5$  M perchloric acid through chronoamperometry. Then, on the as-prepared GCE-graphene-AuNPs, P1 (1  $\mu\text{M}$ ) was self-assembled, and this electrode was treated with 6-mercapto-1-hexanol (1 mM) for 0.5 h. For sensor application, CV was performed over a scan rate range of 50 mV/s, and the potential range was  $0.68$ – $1.42$  V. DPV measurement was also carried out, in which the step potential, pulse amplitude, pulse, scan rate, sampling time and pulse interval were 2 mV, 50 mV, 50 ms, 10 mV/s, 20 ms and 100 ms, respectively.

## 3. RESULTS AND DISCUSSION

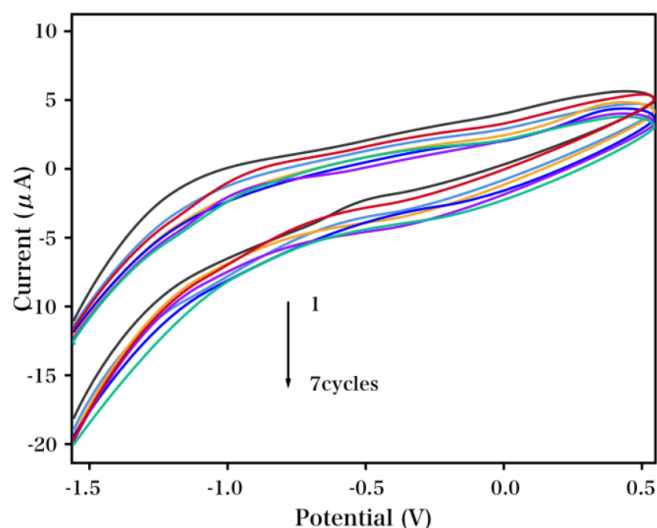


**Figure 1.** (A) CV profiles of the electrodeposition of graphene on a GCE by electrochemically reducing graphene oxide (1.0 mg/mL). Supporting electrolyte: pH 7.0 PBS; Scan rate: 10 mV/s.

The electrodeposition of Au and graphene on a GCE was studied. The electrolysis of graphene oxide on GCE is characterized via cyclic voltammograms in Figure 1A. It can be seen that successive potential scans lead to an increase in the voltammetric current, which suggests that the conductive graphene is deposited on the surface of the GCE. The formation of the graphene-AuNP composite was confirmed using SEM, and the results are shown in Figure 2. Meanwhile, as shown in the SEM image of the GCE surface, graphene was successfully deposited, as confirmed by the observed veli-like film coating [34, 35].

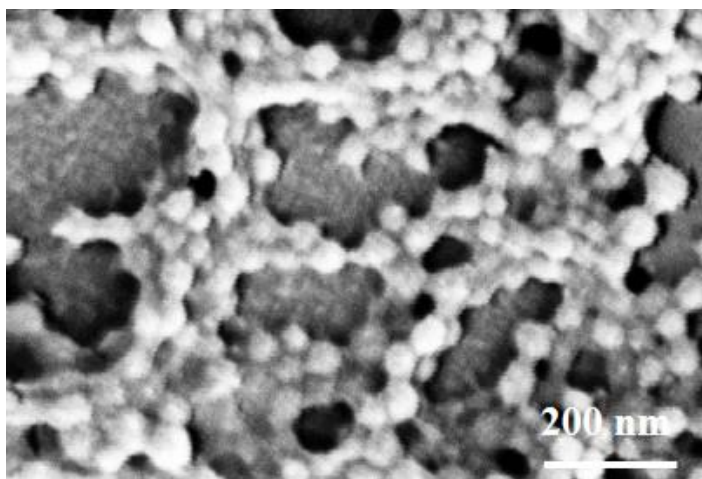


**Figure 2.** SEM image of graphene-AuNPs composite.

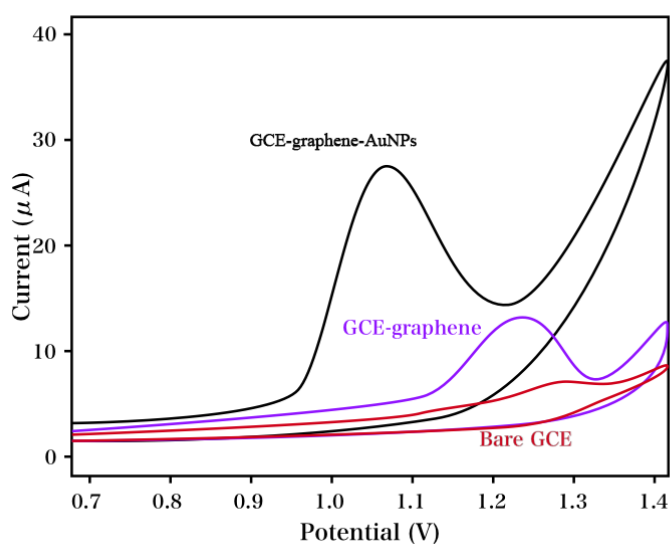


**Figure 3.** CVs profiles of GCE-graphene-AuNPs, bare GCE and GCE-graphene toward 1.0 mM PHD1 (1.0 mM). Supporting electrolyte: pH 7.0 PBS; Scan rate: 50 mV/s.

Electrochemical biosensors provide an attractive resource to analyze the content of a biological sample due to the direct conversion of a biological event to an electronic signal, provided that these are setup properly and reproducibly [36, 37]. CV was performed and recorded for the electrochemical

performance of PHD1 (1.0 mM) using the GCE-graphene-AuNPs at a pH of 7.0 (scan rate: 50 mV/s), where a well-defined anodic peak was observed at *ca.* 1.19 V. Compared with the GCE-graphene and the bare GCE, the GCE-graphene-AuNPs showed a much higher peak intensity (Figure 3). No corresponding reduction peak was found for the reverse scanning, which suggested the irreversibility of the electrode process of PHD1. The voltammograms for the first cycle were generally obtained, and the results indicated the favorable electro-oxidation behavior of the GCE-graphene-AuNPs to PHD1. The excellent selectivity of the proposed electrochemical sensor can be ascribed to the high specific surface area of the graphene-AuNPs, which provide a platform for PHD1 loading [38].

This work also reports the investigation of the potential and accumulation time effects. In the field of electroanalytical chemistry, the detection sensitivity is usually enhanced by open circuit accumulation. As shown in Figure 4, the accumulation time effect on the PHD1 oxidation using the GCE-graphene-AuNPs was studied over a range of 0 to 120 s. As the accumulation time increased from 0 to 70 s, a gradual increase in the peak current was observed. However, when the time exceeded 70 s, an apparent steady state of the current was reached. Thus, 70 s was determined as the optimum accumulation time and was used for the following measurements.

A slight variation was observed for the peak current of PHD1 at different accumulation potentials, which suggested that the peak current of PHD1 was not greatly affected by the accumulation potential. Thus, we performed the accumulation process under open-circuit conditions.

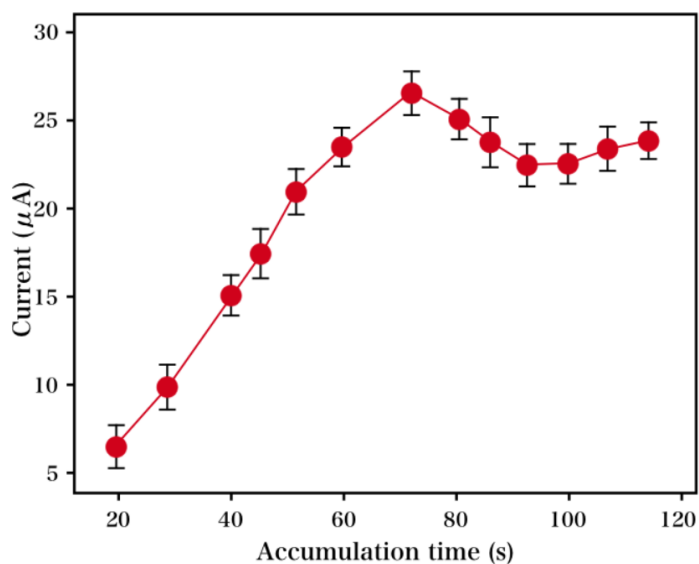


**Figure 4.** Effect of accumulation time on the 1.0 mM PHD1 oxidation using GCE-graphene-AuNPs. Supporting electrolyte: pH 7.0 PBS; Scan rate: 50 mV/s.

The solution pH effect on the electrode reaction was also investigated. Figure 5A shows the CV recorded for the electro-oxidation of PHD1 (1.0 mM) in PBS (pH 4-10). The peak current and potential were greatly affected by the pH of the solution. Briefly, as shown in Figure 5B, the solution pH influenced the peak current and peak potential considerably. With the increase in pH of the solution, the peak potential shifted to less positive values, obeying the following equation:

$$E_p(V) = 1.6406 - 0.0574 \text{ pH}$$

For the above equation, the slope is calculated as 57.4 mV/pH, which is close to 59 mV/pH (expected theoretical value), indicating that the number of hydrogen ions involved in the electrode reaction equals that of the transferred electrons [39]. In the proposed method, the electro-oxidation of PHD1 involves a two electron and two proton transfer process. The C-7 hydroxyl group of PHD1 is more easily oxidized than the C-2 hydroxyl group.

When the pH was 7.0, an increased intensity to a high level was observed, followed by the decrease in peak intensity, as shown in the plot of  $I_{pa}$  vs. pH in Figure 5C. Therefore, pH 7.0 was selected as the optimal pH value, considering that it provided the best sensitivity.

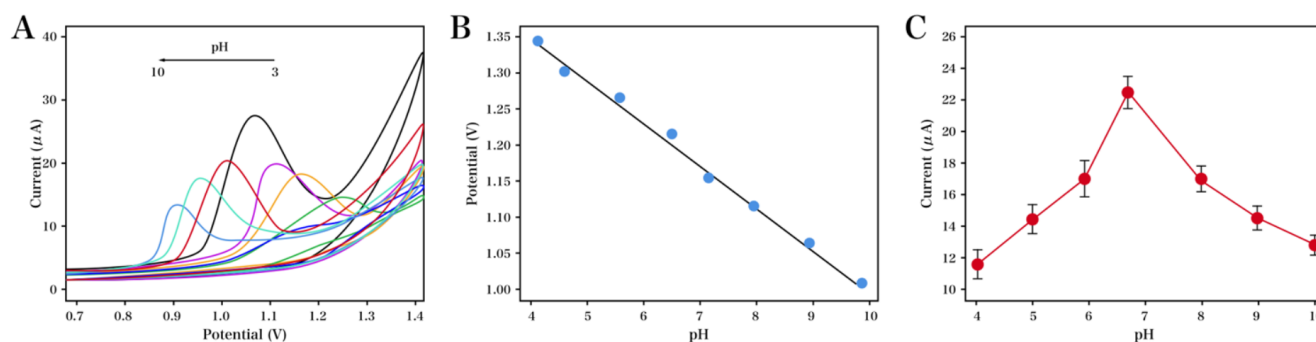


**Figure 5.** (A) CV profiles of 1.0 mM PHD1 oxidation using GCE-graphene-AuNPs under various pH conditions; (B) variations of peak currents  $I_{pa}$  ( $\mu\text{A}$ ) for PHD1; and (C) peak potential  $E_p$  (V) of PHD1.

As shown in Figure 5A, the scan rate effect on the electro-oxidation of PHD1 was studied through linear sweep voltammetry (LSV). As displayed in Figure 5B, a linear range was found between the peak current and the square root of the scan rate over a range of 0.05 to 0.425 V/s, indicating that the currents were typically diffusion controlled. As shown in Figure 5B, the relationship between  $\log v$  and  $\log I_{pa}$  was also linear. The slope value of 0.46 was comparable with the theoretically expected value of 0.5 for a purely diffusion-controlled current, which in turn, confirms that the electro-oxidation of PHD1 was diffusion controlled. A shift toward positive values was found for the peak potential as the scan rate increased, with a linear range of 0.05 to 0.425 V/s, which can be described using the following equation:

$$E_p(\text{V}) = 0.0247 \log v (\text{Vs}^{-1}) + 1.251$$

In terms of this irreversible electrode process, the calculation of  $E_p$  was presented based on Laviron as follows:

$$E_p = E^0 + \left( \frac{2.303RT}{\alpha nF} \right) \log \left( \frac{Rk^0}{\alpha nF} \right) + \left( \frac{2.303RT}{\alpha nF} \right) \log v$$

where  $E^0$  and  $k^0$  are the formal standard redox potential and the standard heterogeneous rate constant of the reaction, respectively;  $\alpha$  and  $n$  are the transfer coefficient and the number of transferred electrons, respectively; and  $v$  refers to the scan rate. The other parameters follow their conventional meanings. The calculation of  $\alpha n$  is based on the slope of the  $E_p$  vs.  $\log v$  plot, where the slope is

0.0259, ( $F = 96480$  C/mol;  $T = 298$  K;  $R = 8.314$  JK/mol). Therefore,  $\alpha n$  can be obtained as 2.2149. According to Bard and Faulkner,  $\alpha$  is calculated using the following equation:

$$\alpha = \frac{47.7}{E_p - E_{p/2}} mV$$

where  $E_{p/2}$  is the potential when the current is at half the peak value, based on which  $\alpha$  can be obtained as 0.9. Additionally,  $n$  during the PHD1 electro-oxidation can be obtained in a range of 2.37  $\sim$  2. From the intercept of the previous plot,  $k^0$  can be calculated with the known  $E^{0'}$  value, which is calculated from the intercept of the  $E_p$  vs.  $v$  curve by extrapolating to the vertical axis at  $v = 0$ . In the present study, the intercept for the  $E_p$  vs.  $\log v$  plot is obtained as 1.2237,  $E^{0'}$  as 1.2087, and  $k^0$  as 1685. In addition, the number of transferred electrons was obtained from the slope of the linear dependency of the anodic peak current on the square root of the potential sweep rate, with the following Randles–Sevcik equation for a completely irreversible charge transfer process:

$$I_{pa} = (2.99 \times 10^5) n \alpha^{1/2} A C_0^* D_0^{1/2} v^{1/2}$$

where  $\alpha$  and  $A$  are the electron transfer coefficient and the electrode area, respectively; and  $C_0^*$  and  $D_0$  are the bulk concentration of the solution and the diffusion coefficient of the electroactive species, respectively. For the GCE-graphene-AuNPs, the electroactive surface area was obtained as  $0.322$  cm<sup>2</sup>. The concentration of the bulk solution and the diffusion coefficient of the electroactive species were obtained as 5 mM and  $6.11 \times 10^{-5}$  cm<sup>2</sup>/s, respectively.

In terms of this irreversible diffusion-controlled process, the calculation of the electron transfer coefficient  $\alpha$  is presented as follows:

$$I_{pa} = 0.227 n F A C^* k^0 \exp\{(-\alpha F / RT)(E_p - E^{0'})\}$$

where  $n$  is the number of electrons transferred,  $I_{pa}$  is the peak current,  $E_p$  is the peak potential,  $E^{0'}$  is the formal redox potential, and  $k^0$  is the heterogeneous rate constant. The value of  $E^{0'}$  is calculated through the extrapolation of the straight line to  $v = 0$  according to the plot of peak potential vs. scan rate. On the other hand,  $\alpha$  is obtained from the plot slope of  $\log I_p$  vs.  $(E_p - E^{0'})$ . In the present study,  $\alpha$  is obtained as 0.5879 (slope: 23.30). Correspondingly, the electron number equals 2.39, and the number of transferred electrons obtained via these two routes is consistent [40].

Considering the poor peaks obtained using CV at a lower PHD1 concentration, the differential-pulse voltammetric measurement was carried out instead for the drug detection. The results confirmed the feasibility of the developed method in the quantitative analysis of PHD1. For the PHD1 quantification, the supporting electrolyte was pH 7.0 PBS in our case due to the maximal peak current shown at this pH. As the PHD1 amount was increased, an increase in the peak current was found (Figure 6A). Using these optimal parameters, linear calibration curves were plotted for PHD1 (0.01 to 2 mM), as shown in Figure 6B. In the case of solutions at higher concentrations, deviation from linearity was found since PHD1 or its oxidation product can be adsorbed on the surface of the electrode. The LOD was obtained as 4  $\mu$ M. Table 1 shows a comparison of the proposed electrochemical sensor with methods reported in the literature. It can be seen that the proposed GCE-graphene-AuNPs exhibit an advanced performance.

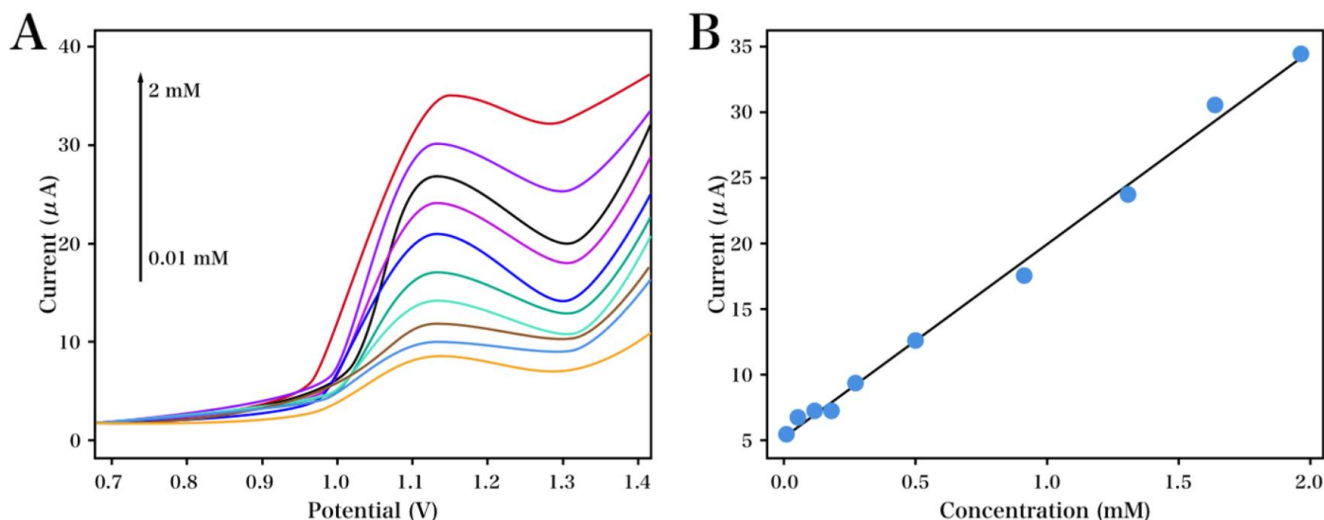


**Figure 6.** (A) Differential pulse voltammograms (DPV) recorded for different PHD1 concentrations using GCE-graphene-AuNPs. Supporting electrolyte: pH 7.0 PBS. Step potential: 2 mV; Pulse amplitude: 50 mV; Pulse: 50 ms, Scan rate: 10 mV/s, Sampling time: 20 ms; Pulse interval: 100 ms. (B) Plot of current vs. PHD1 concentration.

**Table 1.** Comparison of the reported methods and proposed electrochemical sensor for the detection of PHD1.

Methods	Linear detection range	Detection limit	Reference
Spectroscopic detection	-	-	[41]
Nonradioactive 96-well plate assay	0.02 - 50 ng/mL	0.01 ng/mL	[42]
Ferritin-labeled antibodies	0.5-5 mM	-	[43]
GCE-graphene-AuNPs	0.01 - 2 mM	4 μM	This work

**Table 2.** PHD1 analysis in serum specimens (n=3).

Sample	Added (mM)	Found (mM)	Recovery (%)	RSD (%)
1	0	0.144	—	—
2	0.05	0.197	101.55	3.37
3	0.1	0.239	97.95	3.41
4	0.2	0.331	96.22	1.57
5	0.5	0.621	96.42	6.20

Our developed route was further used for the analysis of serum PHD1. The recoveries were measured by injecting PHD1 with a known amount of PHD1. For the quantitative analysis, a standard solution of PHD1 was added to the herb specimens. The analysis of PHD1 injected into the herb specimens was analyzed via the calibration graph. Table 1 shows the LOD and RSD. The recoveries were found to range from 96.22% to 101.55%.

#### 4. CONCLUSIONS

The present study reports the fabrication of GCE-graphene-AuNPs via electrodeposition. This sensor was used for the electrochemical detection of PHD1, with a low LOD of 4  $\mu$ M and a wide linear range of 0.01 mM to 2 mM. Therefore, our developed route has the potential for use in the detection of serum PHD1.

#### References

1. E. Bogaerts, A. Paridaens, X. Verhelst, P. Carmeliet, A. Geerts, H. Van Vlierberghe and L. Devisscher, *Excli Journal*, 15 (2016) 687.
2. M. Ma, S. Hua, G. Li, S. Wang, X. Cheng, S. He, P. Wu and X. Chen, *Oncotarget*, 8 (2017) 12983.
3. M. Schneider, K.V. Geyte, P. Fraisl, J. Kiss, J. Aragonés, M. Mazzone, H. Mairbäurl, K.D. Bock, N.H. Jeoung and M. Mollenhauer, *Gastroenterology*, 138 (2010) 1143.
4. T.G. Smith and N.P. Talbot, *Antioxidants & Redox Signaling*, 12 (2010) 431.
5. S.M. Yun, M.L.M. †, N. Giese, E. Metzen, M.W. Büchler, M.D. Helmut Friess, M.D. Arno Kornberg and P.B.M. ‡, *Cancer*, 118 (2012) 960.
6. N. Fujita, S.S. Gogate, K. Chiba, Y. Toyama, I.M. Shapiro and M.V. Risbud, *Journal of Biological Chemistry*, 287 (2012) 39942.
7. E. Muchnik and J. Kaplan, *Expert Opinion on Investigational Drugs*, 20 (2011) 645.
8. M.H. Rabinowitz, T.D. Barrett, M.D. Rosen and H. Venkatesan, *Annual Reports in Medicinal Chemistry*, 45 (2010) 123.
9. J.R.A. Leushner and J. Pasternak, *Canadian Journal of Zoology*, 56 (2011) 159.
10. S. Kiriakidis, S.S. Hoer, N. Burrows, G. Biddlecome, M.N. Khan, C.C. Thinnis, C.J. Schofield, N. Rogers, M. Botto and E. Paleolog, *Kidney International*, 92 (2017) 900.
11. C.C. Scholz, A.V. Kriegsheim, M.M. Tambuwala, E. Hams, A. Cheong, U. Bruning, P.G. Fallon, E.P. Cummins and C.T. Taylor, *Faseb Journal*, 27 (2013)
12. D.R. Mole, *Antioxidants & Redox Signaling*, 12 (2010) 445.
13. W.A. Denny, *Journal of Medicinal Chemistry*, 55 (2012) 2943.
14. H.F. Ma, T.T. Chen, Y. Luo, F.Y. Kong, D.H. Fan, H.L. Fang and W. Wang, *Microchim. Acta.*, 182 (2015) 2001.
15. M.B. Gholivand, N. Karimian and M. Torkashvand, *Journal of Analytical Chemistry*, 70 (2015) 384.
16. Y. Zhang, R. Sun, B. Luo and L. Wang, *Electrochimica Acta*, 156 (2015) 228.
17. B. Devadas, S. Cheemalapati, S.M. Chen, M.A. Ali and F.M.A. Al-Hemaid, *Ionics*, 21 (2015) 547.
18. J. Wang, B. Yang, H. Wang, P. Yang and Y. Du, *Anal. Chim. Acta.*, 893 (2015) 41.
19. O.M. Istrate, L. Rotariu and C. Bala, *Microchim. Acta.*, 183 (2016) 57.
20. K. Thangavelu, S. Palanisamy, S.M. Chen, V. Velusamy, T.W. Chen and S.K. Ramaraj, *Journal of the Electrochemical Society*, 163 (2016) B726.
21. J. Molina, F. Cases and L.M. Moretto, *Anal. Chim. Acta.*, 946 (2016) 9.
22. L. Fu, G. Lai and A. Yu, *Rsc Advances*, 5 (2015) 76973.
23. R. Feng, X. Hu, C. He, X. Li and X. Luo, *Analytical Letters*, 50 (2017)
24. V. Sharma, D. Hynek, L. Trnkova, D. Hemzal, M. Marik, R. Kizek and J. Hubalek, *Microchim. Acta.*, 183 (2016) 1299.
25. X. Li, A. Zhong, S. Wei, X. Luo, Y. Liang and Q. Zhu, *Electrochimica Acta*, 164 (2015) 203.
26. J. Shan, Y. Liu, R. Li, C. Wu, L. Zhu and J. Zhang, *Journal of Electroanalytical Chemistry*, 738 (2015) 123.
27. A. Abellán-Llobregat, M. Ayán-Varela, L. Vidal, J.I. Paredes, S. Villar-Rodil, A. Canals and E.

- Morallón, *Journal of Electroanalytical Chemistry*, 783 (2016) 41.
28. S. Teixeira, N.S. Ferreira, R.S. Conlan, O.J. Guy and M.G.F. Sales, *Electroanalysis*, 26 (2015) 2591.
29. X. Shen, X. Xia, Y. Du and C. Wang, *Frontiers of Materials Science*, (2017) 1.
30. T. Li, Z. Liu, L. Wang and Y. Guo, *Rsc Advances*, 6 (2016) 30732.
31. X. Chen, D. Zhou, H. Shen, W. Feng, H. Chen and G. Xie, *Farmakologija I Toksikologija*, 4 (2015) 24.
32. Z. Zhao, Y. Sun, P. Li, W. Zhang, K. Lian, J. Hu and Y. Chen, *Talanta*, 158 (2016) 283.
33. W. Zhang, *Journal of Solid State Electrochemistry*, 20 (2016) 499.
34. V. Mani, M. Govindasamy, S.-M. Chen, B. Subramani, A. Sathiyam and J.P. Merlin, *International Journal Of Electrochemical Science*, 12 (2017) 258.
35. K. Movlaee, M.R. Ganjali, M. Aghazadeh, H. Beitollahi, M. Hosseini, S. Shahabi and P. Norouzi, *International Journal of Electrochemical Science*, (2017) 305.
36. A. Peng, H. Yan, C. Luo, G. Wang, Y. Wang, X. Ye and H. Ding, *International Journal Of Electrochemical Science*, 12 (2017) 330.
37. V. Mani, R. Umamaheswari, S.-M. Chen, M. Govindasamy, C. Su, A. Sathiyam, J.P. Merlin and M. Keerthi, *International Journal Of Electrochemical Science*, 12 (2017) 475.
38. Z. Zhong, J. Shan, Z. Zhang, Q. Yi and D. Wang, *Electroanalysis*, 22 (2010) 2569.
39. I. Martins, F.C. Carreira, L.S. Canaes, D.S.C.J. Fa, S.C.L. Da and S. Rath, *Talanta*, 85 (2011) 1.
40. L. Fu, K. Xie, H. Zhang, Y. Zheng, W. Su and Z. Liu, *Coatings*, 7 (2017) 232.
41. L.M. Hoffart, E.W. Barr, R.B. Guyer, J.M. Bollinger and C. Krebs, *Proceedings of the National Academy of Sciences*, 103 (2006) 14738.
42. F. Oehme, W. Jonghaus, L. Narouz-Ott, J. Huetter and I. Flamme, *Analytical Biochemistry*, 330 (2004) 74.
43. B.R. Olsen, R.A. Berg, Y. Kishida and D.J. Prockop, *Science*, 182 (1973) 825

© 2018 The Authors. Published by ESG ([www.electrochemsci.org](http://www.electrochemsci.org)). This article is an open access article distributed under the terms and conditions of the Creative Commons Attribution license (<http://creativecommons.org/licenses/by/4.0/>).